Neurochemistry International 123 (2019) 13–21

Contents lists available at ScienceDirect

Neurochemistry International

journal homepage: www.elsevier.com/locate/neuint

Model systems for analysis of dopamine transporter function and regulation

Moriah J. Hovde, Garret H. Larson, Roxanne A. Vaughan, James D. Foster*

Department of Biomedical Sciences, University of North Dakota, School of Medicine and Health Sciences, Grand Forks, ND, 58202, USA

ARTICLE INFO

Keywords:
Kinetic parameters
Neuronal cultures
CFT
Cholesterol
Striatum
Nucleus accumbens

ABSTRACT

The dopamine transporter (DAT) plays a critical role in dopamine (DA) homeostasis by clearing transmitter from the extraneuronal space after vesicular release. DAT serves as a site of action for a variety of addictive and therapeutic reuptake inhibitors, and transport dysfunction is associated with transmitter imbalances in disorders such as schizophrenia, attention deficit hyperactive disorder, bipolar disorder, and Parkinson disease. In this review, we describe some of the model systems that have been used for *in vitro* analyses of DAT structure, function and regulation, and discuss a potential relationship between transporter kinetic values and membrane cholesterol.

1. Introduction

In the central nervous system the neurotransmitter dopamine (DA) controls many physiological and psychological processes including reward, motivation, attention, and motor activity (Iversen and Iversen, 2007). Dopaminergic neurons located in the substantia nigra and ventral tegmental area regions of the basal gangia project to motor, reward, and cognitive areas such as striatum (Str), nucleus accumbens (NAc), and frontal cortex, where they release DA into synaptic and perisynaptic spaces to mediate these functions. Reuptake of transmitter back into presynaptic neurons serves as the major regulator of DA signaling (Giros et al., 1996) and is mediated by the dopamine transporter (DAT), a plasma membrane protein found exclusively on DA neurons (Nirenberg et al., 1996).

Defects in DA signaling and homeostasis are associated with several neurological disorders including Parkinson disease (PD), schizophrenia, bipolar disorder, depression, and attention-deficit hyperactive disorder (Kristensen et al., 2011; Pramod et al., 2013), and dysregulated DAT function resulting in imbalanced DA levels has been invoked as a potential factor in their etiologies (Hahn and Blakely, 2002; Kristensen et al., 2011; Pramod et al., 2013). DAT is a target for many psychostimulant drugs that suppress reuptake and elevate synaptic DA levels, including addictive compounds such as cocaine and amphetamine (AMPH), and therapeutic drugs prescribed for DA disorders such as Ritalin® (methylphenidate) and Wellbutrin® (bupropion) (Blakely and Bauman, 2000; German et al., 2012; Iversen and Iversen, 2007). DAT can also transport neurotoxic compounds including 6-hydroxydopamine (Miller et al., 1999; Nass et al., 2002), 1-methyl-4-phenylpyridinium (Gainetdinov et al., 1997; Javitch and Snyder, 1984), and environmental chemicals such as paraquat, serving as a gateway for their entry into neurons, a postulated mechanism for dopaminergic neurodegeneration in PD (Miller et al., 1999).

The central role of DAT in signaling, addiction, and disease has made the transporter a focus of intense efforts to elucidate its transport and regulatory mechanisms (Foster and Vaughan, 2017; Kristensen et al., 2011; Rastedt et al., 2017). Such studies are largely undertaken *in vitro* using model systems such as synaptosomes and brain slices, primary neuronal cultures, and cell expression systems (Kristensen et al., 2011; Pramod et al., 2013). In this minireview, we briefly describe the characteristics and scientific and technical advantages and disadvantages of many of these systems, including photomicrographs of several of the described cell lines (Fig. 1), a tabulation of transport and cocaine analog kinetic parameters (Tables 1–4), and discussion of a potential mechanistic link between transporter kinetics and membrane cholesterol (Figs. 2–4).

2. Model systems for studying DAT function and regulation

2.1. Striatal slices

This *ex vivo* system provides the advantage of replicating many aspects of the *in vivo* environment such as tissue architecture, synaptic circuitry, and regulatory machinery. Brains of freshly dispatched animals (commonly rodents) are typically harvested at postnatal days (PND) 3–15, and desired regions of the brain are sliced into 350–500 μm sections that may include cell bodies, projection axons, and terminal regions (Cho et al., 2007; Kearns et al., 2006). However, thicker slices (up to 1 mm) and those from adult rodents have

* Corresponding author. Department of Biomedical Sciences, University of North Dakota School of Medicine and Health Sciences, Grand Forks, ND, 58202, USA.
E-mail address: james.d.foster@med.und.edu (J.D. Foster).

https://doi.org/10.1016/j.neuint.2018.08.015
Received 30 June 2018; Received in revised form 23 August 2018; Accepted 31 August 2018
Available online 01 September 2018

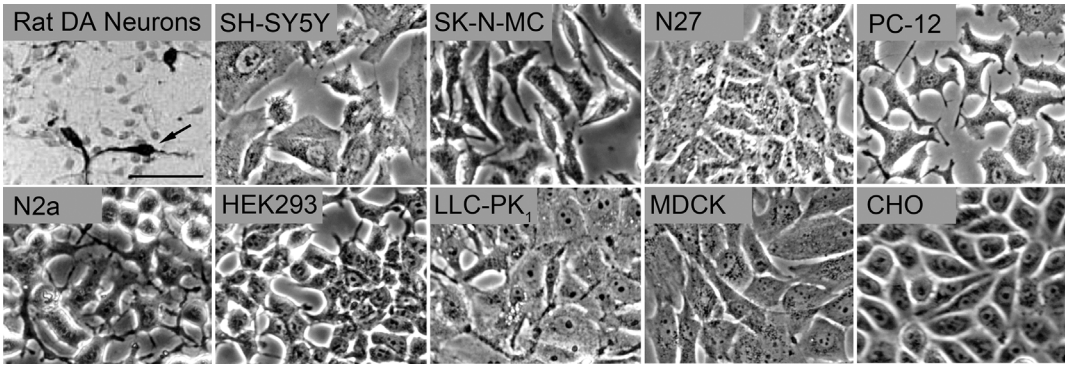

Fig. 1. Morphology of cell systems used to study DAT function and regulation. Panels show phase contrast microscopic images of several cell systems studied in our labs. Images were acquired using a 20X objective on an inverted Olympus microscope equipped with a digital camera. The scale bar indicates 50 μm and is the same for all panels. The dopaminergic neuron image showing tyrosine hydroxylase positive midbrain neurons (arrow) is modified from (Branton and Clarke, 1999).

successfully been used in several studies (Block et al., 2015; Inyushin et al., 2013; Wheeler et al., 2015). The slices are bathed in artificial cerebrospinal fluid and remain viable for many hours, allowing for examination of long-term treatments or outcomes. Sections can be mounted to permeable tissue culture membrane inserts that provide fine access and control, allowing uptake and neuronal functions to be analyzed by high-resolution procedures such fast scan cyclic voltammetry (FSCV) and electrophysiology. Tissue from slices can also be minced or processed into synaptosomes for biochemical analyses.

2.2. Striatal synaptosomes

In this model system desired DA projection areas (usually striatum or NAc) are dissected from brains of freshly dispatched animals and homogenized using a procedure that generates pinched-off, re-sealed nerve terminals. Circuit connections are severed, but the structures retain capacity for transmitter uptake and release, and contain many nerve terminal components including cytoplasm, synaptic vesicles (SVs), mitochondria, receptors, and signaling molecules (Evans, 2018; Whittaker et al., 1964). In terms of monitoring DAT function, synaptosomes have a limited viability (30–60 min), especially after suspension in isotonic medium at physiologic temperature. Transport activity decays considerably across this time frame, possibly due to loss of electrochemical gradient, making synaptosomes suitable primarily for short-term experiments.

2.3. Primary dopaminergic neurons in culture

Primary dopaminergic neurons (typically obtained from mouse or rat embryo midbrain), provide a cell culture system that presumably most closely resembles neurons *in vivo*. The cells express DA markers including tyrosine hydroxylase (TH), DA receptors, and DAT, and contain synaptic vesicles and exocytotic release machinery (Chinta and Andersen, 2005; Choi et al., 2013; Greene, 2006). However, although the harvested neurons are cultured *in vitro* several days prior to use, this may not recapitulate the maturation that occurs *in vivo*. This is an important point for DAT, which undergoes significant developmental regulation. In rats, DAT expression at birth is only ~20–30% of that at PNDs 14–60, and N-linked glycosylation, which regulates DAT processing and targeting, is also negligible at birth (Patel et al., 1994). These properties have not been examined at embryonic stages of development, including those commonly used to obtain primary neurons, and additional DAT regulatory properties including other post-translational modifications (PTMs) and interactome profile have not been characterized at early life stages. In addition, midbrain DA neurons are low in number, constitute only a small fraction of the total neurons present in these regions (see Fig. 1) (Hegarty et al., 2013), and do not undergo cell division, factors which reduce their utility for analyses that require large amounts of uniform source material. However, primary cultures of dopaminergic neurons isolated from *C. elegans*, which can be grown in abundance, have been successfully employed in radiolabeled DA uptake/efflux experiments (Carvelli et al., 2004; Safratowich et al., 2014).

2.4. Human neuroblastoma (SH-SY5Y) cells

The human SH-SY5Y line was subcloned (SK-N-SH → SH-SY → SH-SY5 → SH-SY5Y) from the original line, SK-N-SH, which was isolated in 1970 from a bone marrow biopsy of a 4-year-old girl with neuroblastoma (Biedler et al., 1973). The neuroblast-like cells are slow-growing and only loosely adherent to standard tissue culture plates, making protocols with repeated manipulations such as washing steps problematic due to cell loss. The cells are positive for TH, and produce DA and norepinephrine (NE), but only appear to store DA (Biedler et al., 1978). They also express DAT, the vesicular monoamine transporter 2 (VMAT2), and D_2 and D_3 dopamine receptors, making them a good model for studying the neurotoxic and neuroprotective effects of DA-related compounds (Xicoy et al., 2017). These cells express the norepinephrine transporter (NET), which can also transport DA, necessitating its selective blockade when investigating DAT-mediated DA uptake. The cells also possess cholinergic and GABAergic properties in that they produce acetylcholine and GABA and express muscarinic and nicotinic acetylcholine receptors (Biedler et al., 1978; Kovalevich and Langford, 2013). SH-SY5Y cells express immature neuronal markers, and can be differentiated using a number of methods including retinoic acid, phorbol esters, and dibutyryl cyclic adenosine monophosphate (dbcAMP), with retinoic acid induction being the most commonly used and best-characterized method (Kovalevich and Langford, 2013). After differentiation, SH-SY5Y cells show reduced proliferation, express neuronal markers and become morphologically more similar to primary neurons, with development of neurite processes reminiscent of axons and dendrites (Kovalevich and Langford, 2013).

2.5. Human neuroepithelioma (SK-N-MC) cells

This human neural epithelial line was derived in 1971 from the neuroepithelioma tumor of a 14-year-old girl (Biedler et al., 1973). These neuroblast-like cells are TH-positive and display both catecholaminergic and cholinergic properties (e.g. production of DA, NE, and acetylcholine) (Biedler et al., 1973). They express D_1 but not D_5 DA receptors (Sidhu, 1997), and do not express DAT or NET (Pifl et al., 1996, 1993). The cells grow at a moderate rate and are adherent to standard tissue culture plates. They have a good transfection efficiency and stable expressing clones can be isolated.

2.6. Immortalized rat dopaminergic neurons (N27) cells

The N27 cell line was derived from dopaminergic neurons isolated from embryonic day 14 rat mesencephalon and immortalized with SV40 large T antigen (Prasad et al., 1994). The original lines have been recloned to isolate line 1RB3AN27, with cells that are > 95% TH-positive (Fig. 1) (Prasad et al., 1994). These cells are reported to express TH and DAT mRNA and protein via RT-PCR and immunocytochemistry (Clarkson et al., 1998; Gao et al., 2016). However, they do not display [^{3}H]DA uptake or DAT protein by immunoblotting (Foster and Vaughan, unpublished results), indicating that any endogenous transporter expression is very low and insufficient to support function detectable by typical methodology. They also synthesize and store DA, but lack dopamine-beta-hydroxylase activity and do not synthesize NE (Gao et al., 2016). N27 cells can be differentiated using dbcAMP plus dehydroepiandrosterone (Clarkson et al., 1998). After differentiation, the cells become morphologically more similar to primary neurons, with production of neurite processes and increased TH and DAT mRNA levels. It is reported that after many passages TH expression becomes highly variable (Gao et al., 2016), and these cells require further analysis to assess their dopaminergic character. The N27 line has recently been recloned, producing line N27-A, in which nearly 100% of the cells express TH, and DAT levels increase 3–4 fold (Gao et al., 2016). N27-A cells also express VMAT2, dopaminergic transcription factors Nurr1, En1, FoxA2 and Pitx3 (Gao et al., 2016), and show DA release under basal and depolarizing conditions (Gao et al., 2016). The cells grow at a moderate rate and are strongly adherent to standard tissue culture plates. They have a good transfection efficiency and stable expressing clones can be isolated.

2.7. Rat adrenal gland pheochromocytoma (PC-12) cells

This cell line was derived from a rat pheochromocytoma adrenal gland transplantable tumor (Greene and Tischler, 1976). They are small, irregularly shaped cells (see Fig. 1) that are slow-growing and weakly adherent to standard tissue culture plates, making protocols with repeated manipulations problematic. The cells are catecholaminergic, producing and storing DA and NE but not epinephrine (Greene and Rein, 1977; Greene and Tischler, 1976). PC-12 cells respond reversibly to nerve growth factor (NGF), which induces neurite outgrowth when plated on collagen-coated culture flasks (Greene and Tischler, 1976). The cells express little to no endogenous DAT, but transporter expression increases upon differentiation (Greene and Tischler, 1976). The cells also express NET, which must be selectively blocked for analysis of DAT-dependent DA uptake. They have a moderate transfection efficiency and stable expressing clones can be isolated.

2.8. Mouse neuroblastoma Neuro-2a (N2a) cells

This neuronal line was derived from a mouse neuroblastoma tumor and has been widely used for studies of neurite outgrowth and neurotoxicity (Salto et al., 2015). They do not endogenously express DAT or other monoamine transporters and are not known to synthesize or store monoamine neurotransmitters, but can be differentiated using dbcAMP into cells possessing neuronal properties such as neurite extensions, increased TH expression, and ability to synthesize DA (Tremblay et al., 2010). The cells are fast-growing and adherent to standard tissue culture plates, have a good transfection efficiency, and stable expressing clones can be isolated.

2.9. Human embryonic kidney 293 (HEK293) cells

This line was derived from adenovirus transformation of human embryonic kidney cells. They have an endothelial morphology (Fig. 1), although the cells possess some properties of immature neurons such as expression of neurofilament proteins (Louis et al., 1997; Shaw et al., 2002). They are a widely used, fast-growing line with very high transfection efficiency, but are weakly adherent to standard tissue culture plates and easily dislodged, making protocols with repeated manipulations problematic. To overcome this issue the more tightly adherent GripTite™ 293 MSR (Invitrogen) cell line was developed in which the HEK293 line was engineered to express the human macrophage scavenger receptor to increase cell adherence (Robbins and Horlick, 1998).

2.10. Lilly laboratories cell porcine kidney (LLC-PK$_1$) cells

In recent years, this LLC cell line has been commonly misidentified as a Lewis Lung Carcinoma, but was established in 1958 at Lilly Research Laboratories from the kidneys of a domestic male Hampshire pig (Hull et al., 1976). They are a spontaneously-immortalized epithelial line that is fast-growing and strongly adherent to standard tissue culture plates, making them advantageous for use in protocols with repeated manipulations. They are also very stable, undergoing little to no transformation or neoplastic change after numerous passages. In fact, the original line was passaged 88 times before first being frozen and stored in liquid nitrogen (Hull et al., 1976). The cells have a moderate transfection efficiency and stable expressing clones can be isolated.

2.11. Madin darby canine kidney (MDCK) cells

This cell line was established in 1958 from the kidney of a normal adult female cocker spaniel by S.H. Madin and N.B. Darby (Leighton et al., 1970). They are a spontaneously-immortalized epithelial cell line that is fast-growing and strongly adherent to standard tissue culture plates making them advantageous for protocols with repeated manipulations. These cells have a moderate transfection efficiency and are a widely used heterologous expression model (Leighton et al., 1970).

2.12. CV-1 in origin carrying SV40 (COS-7) cells

This fibroblast-like cell line was derived in the 1980s from transformation of normal CV-1 cells obtained from the kidney of an African green monkey. CV-1 cells were transformed using a mutant strain of the SV40 virus which produces large wild-type T-antigen resulting in the COS-7 line (Gluzman, 1981). They are fast-growing, adherent cells that have good transfection efficiency and are commonly used for recombinant mammalian protein expression (Aruffo, 2002).

2.13. Chinese hamster ovary (CHO) cells

These epithelial cells were derived from ovaries of Chinese hamsters. They are a commonly used model with multiple distinct lines (CHO-K1, CHO-DXB11, CHO-pro3) possessing different attributes derived from the original (Lai et al., 2013; Wurm, 2004). They are fast-growing adherent cells having high transfection efficiency and the ability to produce significant levels of recombinant proteins (Lai et al., 2013; Wurm, 2004).

3. Transport and binding kinetic parameters in various model systems

In Tables 1–4 we have collated kinetic parameters for DAT transport (K_m and V_{max}) and cocaine analog binding (K_d and B_{max}) reported from many of these commonly used model systems. Most of the reported findings were obtained from studies using mouse, rat, monkey, and human brain tissues, or cell systems heterologously expressing cloned transporters from these species. The tables include only results obtained with WT or epitope-tagged transporters under control conditions, and do not include outcomes related to experimental manipulations or mutations. We acknowledge that this tabulation may not be fully

Table 1
V_{max} and K_m values determined for DA transport in various cell lines.

Cell Lines	V_{max} *(pmol/min/mg)*	K_m *(μM)*	Reference
rDAT			
LLC-PK_1	300–1925	1.5–5.2	(Foster et al., 2012; Foster and Vaughan, 2011; Gu et al., 1994)
COS-7	0.004–147	1.5–3.5	(Dar et al., 2006, 2005; Lee et al., 1996; Lin et al., 2000; Mazei-Robison and Blakely, 2005)
CHO	348 ± 22	1.7 ± 0.3	(Morón et al., 2003)
mDAT			
MDCK	–	2.0 ± 0.3	(Wu and Gu, 1999)
rmkDAT			
HEK	14.4[a]	2.9	(Kaufman and Madras, 1993)
hDAT			
Oocytes	6–66[b]	7–8	(Doolen and Zahniser, 2001; Mayfield et al., 2001; Zhu et al., 1997)
LLC-PK_1	4.5 ± 1.2	0.8 ± 0.1	(Zhen and Reith, 2016)
MDCK	–	2.4 ± 0.4	(Wu and Gu, 1999)
C17.2[c]	180 ± 5	5 ± 1	(Grammatopoulos et al., 2010)
CHO	1.0–15.7[a]	0.7–2.2	(Cartier et al., 2015; Hamilton et al., 2015; Midde et al., 2015; Slusher et al., 1997)
N27	99 ± 18	2.8 ± 0.4	(Wu et al., 2017)
HEK[d]	0.2–61.2	0.1–2.6	(Carvelli et al., 2002; Chen et al., 2003, 2000; 1999; Guptaroy et al., 2011; Jones et al., 2012; Li et al., 2017)
N2a	5.5–6.9	0.4–4.3	(Mikelman et al., 2017; Zhang et al., 1998)
PC12	6.9–12.4[a]	1.3–4.8	(Huang et al., 1999; Melikian and Buckley, 1999; Yuan et al., 2016)
SH-SY5Y	2.1–8.9	0.4–1.4	(Bermingham et al., 2017; Hara et al., 2013; Jiang et al., 2004)
SK-N-MC	45 ± 88	1.1–1.2	(Pifl et al., 1993; Sweeney et al., 2017)

[a] pmol/min/10^5 cells.
[b] fmol/sec.
[c] Mouse multipotent neural progenitor cells.
[d] Some FLAG tagged.

comprehensive but hope that the information will serve as a useful resource for DAT investigators.

3.1. K_m and V_{max} for DA transport

DAT transport parameters are typically determined *in vitro* by [^{3}H]-DA uptake saturation analysis, although kinetic constants can also be obtained non-isotopically by rotating disc electrode voltammetry (Jones et al., 2012; Volz et al., 2009). Uptake activity in live animals or brain slices can be measured with FSCV (Cremona et al., 2011; Ferris et al., 2014; Garcia-Olivares et al., 2013; Speed et al., 2011; Wheeler et al., 2017), microdialysis (Howell and Wilcox, 2002), or assessed indirectly by detection of substrate-driven ion currents (Sulzer et al., 2005; Tang et al., 2015), but these methods are less amenable for saturation analyses needed to derive kinetic constants.

A compilation of K_m and V_{max} values for DA transport in various cell lines and tissue preparations is shown in Tables 1 and 2, with K_m values displayed as scatterplots in Fig. 2. It can be seen that even for studies performed with the same species or in the same system there is a certain amount of variability. However, a major pattern that emerges is that K_m for DATs expressed in the brain is up to 10-fold lower (30–500 nM) than for transporters expressed heterologously (0.1–5 μM) (Fig. 2).

For studies performed with brain tissue there were no significant K_m differences between species, brain regions, or tissue preparation method. The few values available for human DAT were similar to those obtained from other species, although these studies may include caveats such as differential post-mortem intervals and tissue freezing that could impact uptake parameters. In cell culture systems there were no clear differences in K_m values between cell types, although we cannot exclude that minor differences might be obscured by variability.

Maximal uptake velocities, V_{max}, also show considerable variability. In this case it is virtually impossible to mechanistically interpret the

Table 3
B_{max} and K_d values for CFT binding determined for DAT in various cell lines.

Cell Lines	CFT B_{max} *(fmol/mg)*	CFT K_d *(nM)*	Reference
rDAT			
LLC-PK_1	681–804[a]	32–77	(Moritz et al., 2013)
COS-7	7000	4–22	(Eshleman et al., 1995; Kitayama et al., 1992)
hDAT			
LLC-PK_1	2000 ± 200	22 ± 3	(Zhen and Reith, 2016)
CHO	5–10[b]	8–9	(Midde et al., 2015; Slusher et al., 1997)
HEK	1000–13,000	16–22	(Berfield et al., 1999; Chen et al., 2000; Wang et al., 2003; Zhen et al., 2015, 2005)
N2a	2500 ± 300	19–22	(Little et al., 2002; Zhang et al., 1998)
SK-N-MC	–	18 ± 4	(Sweeney et al., 2017)

[a] fmol/well.
[b] pmol/10^5 cells.

Table 2
V_{max} and K_m values determined for DA transport in animal tissues and brain regions.

Tissue Type/Region	V_{max} *(pmol/min/mg)*	K_m *(μM)*	Reference
Rat			
Striatal Synaptosomes (including NAc and CPu)	6–159	0.03–0.50	(Afonso-Oramas et al., 2009; Carvelli et al., 2002; Foster and Vaughan, 2011; Hong and Amara, 2010; Jones et al., 2017; Moritz et al., 2013; Morón et al., 2003; Richards and Zahniser, 2009; Vaughan et al., 1997; Zahniser et al., 1999)
VTA Slices	0.33 ± 0.03[a]		(Mebel et al., 2012)
Striatum (*in vivo*)	0.7[a]	10–12 (K_T)	(Sabeti et al., 2002; Zahniser et al., 1999)
Mouse			
Striatal Synaptosomes	38 ± 7	0.06 ± 0.01	(Rao et al., 2013)
NAc Slices	1.0[a]	0.2	(Lu et al., 2015)
Human			
Striatal Synaptosomes		0.41	(Mash et al., 2002)
Drosophila			
Channelrhodospin2 (ChR2) DA neurons	0.11 ± 0.02[a]	1.3 ± 0.6	(Vickrey et al., 2013)

[a] μM/s.

Table 4
B_{max} and K_d values for β-CFT binding determined for DAT in animal tissues.

Tissue Type/Region	CFT B_{max} *(fmol/mg)*	CFT K_d *(nM)*	Reference
Rat			
Striatal Synaptosomes (including NAc and CPu)	61–1950	7–63	(Foster et al., 2008; Hong and Amara, 2010; Jones et al., 2017; Kimmel et al., 2000; Moritz et al., 2013; Woolverton et al., 2000; Zhen et al., 2005)
Mouse			
Striatal Synaptosomes	3700 ± 800	5 ± 1	(Rao et al., 2013)
Rhesus Monkeys (*Macaca mulatta*)			
Striatal Synaptosomes (including NAc and CPu)	753–1850	1–27	(Beveridge et al., 2009; Kaufman and Madras, 1993; Letchworth et al., 2001; Madras et al., 1989; Woolverton et al., 2000)
Human			
Frozen CPu Synaptosomes	10,000 ± 400	4 ± 1	(Staley et al., 1994)
Frozen CPu Synaptosomes	6 ± 4[a]	12 ± 2[a]	(Little et al., 1993)
Frozen NAc Synaptosomes	6 ± 3[a]	8 ± 1[a]	(Little et al., 1993)

[a] *nCi*/mg.

differences, as velocity depends on surface expression of the transporter, which can vary greatly between systems and studies. Interpretation of V_{max} values can be performed within studies if velocities are normalized for DAT surface expression, and in controlled characterizations V_{max} has been shown to be responsive to regulatory manipulations (Bermingham et al., 2017; Foster and Vaughan, 2011; Kivell et al., 2014; Moritz et al., 2015).

3.2. K_d and B_{max} for β-CFT binding

Several radioligands based on transporter blockers have been used to assess DAT binding functionality, including [^{3}H]GBR 12909, [^{3}H] mazindol, and [^{125}I]RTI 55, but arguably the most commonly used ligand for these types of analysis is the cocaine analog [^{3}H] β-CFT (2-beta-carbomethoxy-3-beta-(4-fluorophenyl) tropane). A compilation of K_d and B_{max} values for [^{3}H]β-CFT binding is shown in Tables 3 and 4. $K_{d(β\text{-}CFT)}$ ranged from 4 to 77 nM in cell lines and from 1 to 63 nM in brain tissue. Comparison of mean values obtained from synaptosomes (16 ± 5 nM) to those of cell systems showed statistical difference only for LLC-PK_1 cells (44 ± 17 nM, $p < 0.05$).

The maximal number of β-CFT binding sites, B_{max}, vary widely between studies, and as for V_{max}, are virtually impossible to compare unless the experiments are conducted under identical conditions and values normalized for DAT expression.

4. Potential mechanisms for kinetic differences between systems

The general similarities of DAT kinetic and biochemical properties in these model systems supports their utility for many types of analyses. However, the finding that kinetic parameters differ for native and heterologously expressed DATs suggests subtle but detectable impacts of system properties on the conformational equilibrium of the protein. During the transport process DAT cycles through multiple conformational states, including outwardly-facing forms that bind extracellular DA, occluded forms generated by extracellular and intracellular gates that control the directionality of substrate movement, inward forms that release substrate to the cell interior, and reorientation of the empty protein back to the outward form for another round of transport (Forrest and Rudnick, 2010; Krishnamurthy et al., 2009; Shimamura et al., 2010). The overall rate of these events defines V_{max}, and K_m represents the summation of the kinetic rates between these and other likely intermediate forms. These events also pertain to actions of uptake inhibitors, as the outwardly-facing transporter is the preferred conformation for cocaine analog binding (Beuming et al., 2006; Dahal et al., 2014; Krout et al., 2017), while atypical inhibitors may prefer inwardly facing forms (Loland et al., 2008; Reith et al., 2012; Schmitt and Reith, 2011).

Multiple processes control these events, including interactions with regulatory binding partners, post-translational modifications, and cholesterol and membrane raft partitioning (Kristensen et al., 2011; Vaughan and Foster, 2013), and it is likely that differences between brain and cell systems in one or more of these parameters could underlie differential transport kinetics.

For example, several proteins including syntaxin 1A, flotillin 1, DA receptors, and G protein subunits bind to cytoplasmic domains of DAT mechanistically linked to the permeation pathway to regulate forward

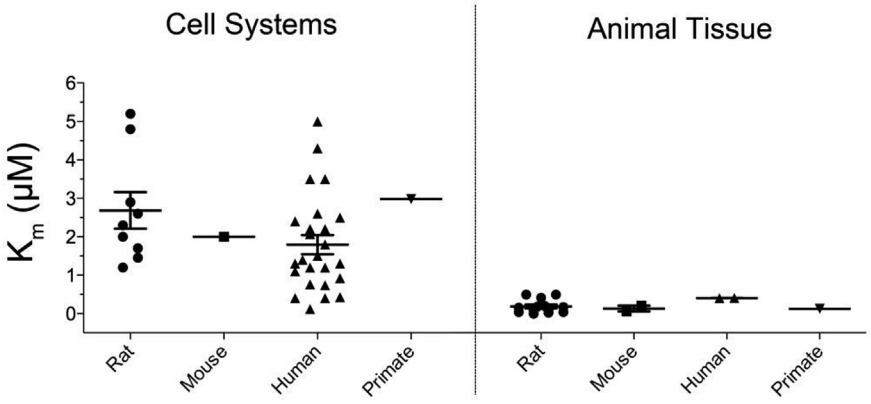

Fig. 2. Distribution of $K_{m(DA)}$ values across model systems. Scatterplot representation of reported $K_{m(DA)}$ values for rat, mouse, human, and nonhuman primate DATs expressed in cell or brain tissue systems.

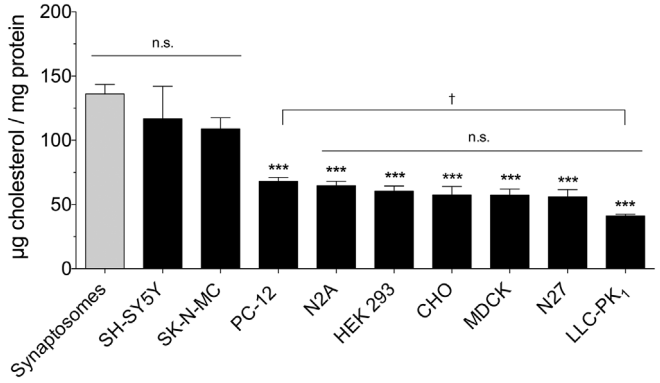

Fig. 3. Membrane cholesterol content from DAT model systems. Membranes were prepared as previously described from cells (Moritz et al., 2013) or rat striatal synaptosomes (Foster and Vaughan, 2011) and assayed for total cholesterol using a colorimetric total cholesterol kit from Fujifilm Wako Diagnostics (Richmond, VA) and total protein using the BCA method as previously described (Foster et al., 2008). Values shown are means ± SEM (n = 3–6). Statistical analysis was performed by ANOVA with a Dunnett's multiple comparison post-hoc test. ***, $p < 0.001$ indicated cells vs. synaptosomes; †, $p < 0.05$ PC-12 cells vs. LLC-PK$_1$ cells; n. s. no statistical difference for indicated groupings.

and reverse transport, and cell models, especially those with few neuronal characteristics, may lack appropriate expression of these partners (Kristensen et al., 2011; Vaughan and Foster, 2013). It has also been postulated that in neurons, translocation of DA across the plasma membrane is directly coupled to transmitter loading into SVs by VMAT2 (Cartier et al., 2010; Egana et al., 2009). This could enhance transport and/or suppress constitutive efflux by reducing levels of free intracellular DA that could re-bind to inwardly-facing transporter forms, with differential impacts on these properties in cells that lack VMAT2 or SVs.

In addition, DAT is tightly regulated by multiple kinase pathways, with N- and C-terminal domains containing sites of phosphorylation and palmitoylation that mediate some of these events (Foster and Vaughan, 2017; Kristensen et al., 2011; Ramamoorthy et al., 2011; Rastedt et al., 2017). Signaling pathways are known to be altered in immortalized and cancer cell lines (Hanahan and Weinberg, 2011), and model systems may lack the repertoire of enzymes and signals that perform these functions in neurons. We have previously noted differences in DAT glycosylation, phosphorylation, and palmitoylation characteristics between different brain regions and between brain and cell systems (Foster et al., 2003; Foster and Vaughan, 2011; Lew et al., 1992), supporting this idea.

Membrane cholesterol is also key to DAT function, with transport activity being reduced or enhanced, respectively, by depletion or supplementation of cholesterol (Adkins et al., 2007; Foster et al., 2008; Hong and Amara, 2010; Jones et al., 2012). These effects may be exerted by direct sterol interaction with DAT (Penmatsa et al., 2015; Wang et al., 2015; Zeppelin et al., 2018) or by impacts on DAT partitioning to cholesterol-rich membrane rafts that control DAT interactome, phosphorylation, and conformational equilibrium (Adkins et al., 2007; Cremona et al., 2011; Foster et al., 2008; Hong and Amara, 2010; Jones et al., 2012).

To examine the possibility that the kinetic differences reported between brain and cell systems relate to cholesterol/DAT relationships, we measured membrane cholesterol from several of the model systems available in our labs (Fig. 3). The results show about a 3-fold range in cholesterol content, with highest levels in rat striatal synaptosomes and the neuronally-derived cell lines SH-SY5Y and SK-N-MC (109–136 µg/mg protein; $p < 0.001$ vs LLC-PK$_1$ cells), an intermediate level in PC-12 cells (68 µg/mg protein $p < 0.05$ vs LLC-PK$_1$ cells, $p < 0.001$ vs striatal synaptosomes), and lowest levels in the remaining cells (41–57 µg/mg protein, $p < 0.001$ vs striatal synaptosomes) (Fig. 3). Correlation analysis (Fig. 4A) revealed a statistically significant inverse relationship between membrane cholesterol and $K_{m(DA)}$ ($r^2 = 0.78$, $^{**}p = 0.0008$), consistent with enhancement of transport. We found no significant correlation across all cell lines between cholesterol and $K_{d(\beta\text{-CFT})}$ ($r^2 = 0.16$, $p = 0.43$) (Fig. 4B), although binding affinities did differ between LLC-PK$_1$ cells and synaptosomes, the systems with the greatest difference in cholesterol content. The apparent ability of cholesterol to affect $K_{m(DA)}$ but not $K_{d(\beta\text{-CFT})}$ could indicate that the impact follows from alteration of conformational movements during the transport cycle rather than stabilization of a particular transporter form. These findings thus identify an endogenous biochemical difference between model cells and native tissues that may relate to transport mechanisms.

5. Conclusions

The relative similarities of transport and binding values obtained in these model systems indicates their general usefulness for many types of studies on DAT structure and function. Primary neurons and cells that endogenously express DAT and other DA machinery may be more suited for regulatory studies and analyses that use approaches such as imaging and electrophysiology that do not require large numbers of cells. Heterologous expression systems that can generate higher levels of the transporter may be more suited for biochemical or protein isolation analyses but may not faithfully recapitulate neuronal regulatory events that can impact functional outcomes. Such issues are key for interpretation of transporter alterations in disease and drug abuse, and will be aided by continuing elucidation of DAT characteristics.

Conflicts of interest

The authors declare no conflicts of interest.

Acknowledgements

Work from the authors' laboratories was supported by grants from the National Institutes of Health DA031991 (JDF), DA13147 and P20-GM104360 (RAV), P30-GM103329 (UND), P20-GM12345 (UND).

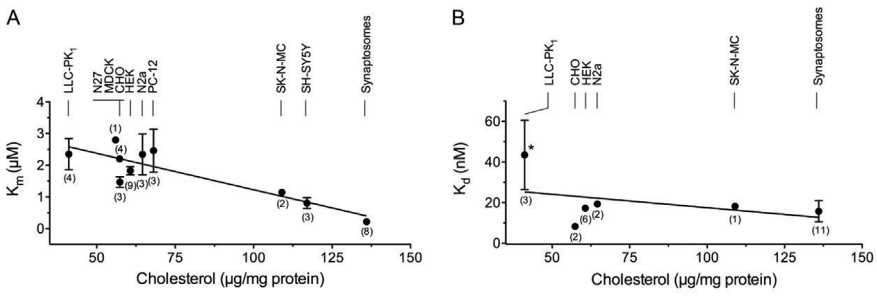

Fig. 4. Inverse correlation between K_m and membrane cholesterol content. (A) Plot of pooled $K_{m(DA)}$ values (means ± SEM) vs. membrane cholesterol for the indicated cell lines and tissues. The line indicates the linear regression analysis ($r^2 = 0.78$; Pearson correlation coefficient of $r = -0.88$; $^{***}p = 0.0008$). (B) Plot of $K_{d(CFT)}$ values (means ± SEM) vs. membrane cholesterol for the indicated cell lines and tissues. The line indicates linear regression analysis ($r^2 = 0.16$, Pearson correlation coefficient of $r = -0.4$; $p = 0.43$). Asterisk indicates significant difference (*, $p < 0.05$) between $K_{d(CFT)}$ LLC-PK$_1$ vs synaptosomes. Numbers in parentheses indicate the number of reports for each system and where absent error bars lie within the symbol.

References

Adkins, E.M., Samuvel, D.J., Fog, J.U., Eriksen, J., Jayanthi, L.D., Vaegter, C.B., Ramamoorthy, S., Gether, U., 2007. Membrane mobility and microdomain association of the dopamine transporter studied with fluorescence correlation spectroscopy and fluorescence recovery after photobleaching. Biochemistry 46, 10484–10497.

Afonso-Oramas, D., Cruz-Muros, I., de la Rosa, D.Á., Abreu, P., Giráldez, T., Castro-Hernández, J., Salas-Hernández, J., Lanciego, J.L., Rodríguez, M., González-Hernández, T., 2009. Dopamine transporter glycosylation correlates with the vulnerability of midbrain dopaminergic cells in Parkinson's disease. Neurobiol. Dis. 36, 494–508.

Aruffo, A., 2002. Expression of proteins in mammalian cells: transient expression of proteins. Basic Protoc. Protein Expr. 1–7.

Berfield, J.L., Wang, L.C., Reith, M.E.A., 1999. Which form of dopamine is the substrate for the human dopamine Transporter : the cationic or the uncharged species. J. Biol. Chem. 274, 4876–4882.

Bermingham, D.P., Hardaway, J.A., Refai, O., Marks, C.R., Snider, S.L., Sturgeon, S.M., Spencer, W.C., Colbran, R.J., Miller, D.M., Blakely, R.D., 2017. The atypical MAP kinase SWIP-13/ERK8 regulates dopamine transporters through a Rho-dependent mechanism. J. Neurosci. 37, 9288–9304.

Beuming, T., Shi, L., Javitch, J., Weinstein, H., 2006. A comprehensive structure-based alignment of prokaryotic and eukaryotic neurotransmitter/Na+ symporters (NSS) aids in teh use of the LeuT structure to probe NSS structure function. Mol. Pharmacol. 70, 1630–1642.

Beveridge, T.J.R., Smith, H.R., Nader, M.A., Porrino, L.J., 2009. Abstinence from chronic cocaine self-administration alters striatal dopamine systems in rhesus monkeys. Neuropsychopharmacology 34, 1162–1171.

Biedler, J., Helson, L., Spengler, B., 1973. Morphology and growth, tumorigenicity, and cytogenetics of human neuroblastoma cells in continuous culture. Canc. Res. 33, 2643–2652.

Biedler, J., Roffler-Tarlov, S., Schachner, M., Freedman, L., 1978. Multiple neurotransmitter synthesis by human neuroblastoma cell lines and clones. Canc. Res. 38, 3751–3757.

Blakely, R.D., Bauman, A.L., 2000. Biogenic amine transporters: regulation in flux. Curr. Opin. Neurobiol. 10, 328–336.

Block, E.R., Nuttle, J., Balcita-Pedicino, J.J., Caltagarone, J., Watkins, S.C., Sesack, S.R., Sorkin, A., 2015. Brain region-specific trafficking of the dopamine transporter. J. Neurosci. 35, 12845–12858.

Branton, R.L., Clarke, D.J., 1999. Apoptosis in primary cultures of E14 rat ventral Mesencephala : time course of dopaminergic cell death and implications for neural transplantation. Exp. Neurol. 98, 88–98.

Cartier, E., Hamilton, P.J., Belovich, A.N., Shekar, A., Campbell, N.G., Saunders, C., Andreassen, T.F., Gether, U., Veenstra-Vanderweele, J., Sutcliffe, J.S., Ulery-Reynolds, P.G., Erreger, K., Matthies, H.J.G., Galli, A., 2015. Rare autism-associated variants implicate syntaxin 1 (STX1 R26Q) phosphorylation and the dopamine transporter (hDAT R51W) in dopamine neurotransmission and behaviors. EBioMedicine 2, 135–146.

Cartier, E.A., Parra, L.A., Baust, T.B., Quiroz, M., Salazar, G., Faundez, V., Egaña, L., Torres, G.E., 2010. A biochemical and functional protein complex involving dopamine synthesis and transport into synaptic vesicles. J. Biol. Chem. 285, 1957–1966.

Carvelli, L., McDonald, P.W., Blakely, R.D., DeFelice, L.J., 2004. Dopamine transporters depolarize neurons by a channel mechanism. Proc. Natl. Acad. Sci. U.S.A. 101, 16046–16051.

Carvelli, L., Moron, J.A., Kahlig, K.M., Ferrer, J.V., Sen, N., Lechleiter, J.D., Leeb-lundberg, F.L.M., Merrill, G. a, Lafer, E.M., Ballou, L.M., Shippenberg, T.S., Javitch, J.A., Lin, R.Z., Galli, A., 2002. PI 3-kinase regulation of dopamine uptake. J. Neurochem. 81, 859–869.

Chen, N., Appell, M., Berfield, J.L., Reith, M.E.A., 2003. Inhibition by arachidonic acid and other fatty acids of dopamine uptake at the human dopamine transporter. Eur. J. Pharmacol. 478, 89–95.

Chen, N., Ferrer, J.V., Javitch, J.A., Justice, J.B., 2000. Transport-dependent accessibility of a cytoplasmic loop cysteine in the human dopamine transporter. J. Biol. Chem. 275, 1608–1614.

Chen, N., Trowbridge, C.G., Justice, J.B., 1999. Cationic modulation of human dopamine transporter: dopamine uptake and inhibition of uptake. J. Pharmacol. Exp. Therapeut. 290, 940–949.

Chinta, S.J., Andersen, J.K., 2005. Dopaminergic neurons. Int. J. Biochem. Cell Biol. 37, 942–946.

Cho, S., Wood, A., Bowlby, M., 2007. Brain slices as models for neurodegenerative disease and screening platforms to identify novel therapeutics. Curr. Neuropharmacol. 5, 19–33.

Choi, W.-S., Kim, H.-W., Xia, Z., 2013. Preparation of primary cultured dopaminergic neurons from mouse brain. Neural Dev. 61–69.

Clarkson, E.D., Rosa, F.G., Edwards-Prasad, J., Weiland, D.A., Witta, S.E., Freed, C.R., Prasad, K.N., 1998. Improvement of neurological deficits in 6-hydroxydopamine-lesioned rats after transplantation with allogeneic simian virus 40 large tumor antigen gene-induced immortalized dopamine cells. Proc. Natl. Acad. Sci. U.S.A. 95, 1265–1270.

Cremona, L.M., Matthies, H.J.G., Pau, K., Bowton, E., Speed, N., Lute, B.J., Anderson, M., Sen, N., Robertson, S.D., Vaughan, R.A., Rothman, J.E., Galli, A., Javitch, J.A., Yamamoto, A., 2011. Flotillin-1 is essential for PKC-triggered endocytosis and membrane microdomain localization of DAT. Nat. Neurosci. 14, 469–477.

Dahal, R.A., Pramod, A.B., Sharma, B., Krout, D., Foster, J.D., Cha, J.H., Cao, J., Newman, A.H., Lever, J.R., Vaughan, R.A., Henry, L.K., 2014. Computational and biochemical docking of the irreversible cocaine analog RTI 82 directly demonstrates ligand positioning in the dopamine transporter central substrate-binding site. J. Biol. Chem. 289, 29712–29727.

Dar, D.E., Mayo, C., Uhl, G.R., 2005. The interaction of methylphenidate and benztropine with the dopamine transporter is different than other substrates and ligands. Biochem. Pharmacol. 70, 461–469.

Dar, D.E., Metzger, T.G., Vandenbergh, D.J., Uhl, G.R., 2006. Dopamine uptake and cocaine binding mechanisms: the involvement of charged amino acids from the transmembrane domains of the human dopamine transporter. Eur. J. Pharmacol. 538, 43–47.

Doolen, S., Zahniser, N.R., 2001. Protein tyrosine kinase inhibitors alter human dopamine transporter activity in Xenopus oocytes. J. Pharmacol. Exp. Therapeut. 296, 931–938.

Egana, L.A., Cuevas, R.A., Baust, T.B., Parra, L.A., Leak, R.K., Hochendoner, S., Pena, K., Quiroz, M., Hong, W.C., Dorostkar, M.M., Janz, R., Sitte, H.H., Torres, G.E., 2009. Physical and functional interaction between the dopamine transporter and the synaptic vesicle protein Synaptogyrin-3. J. Neurosci. 29, 4592–4604.

Eshleman, A.J., Neve, R.L., Janowsky, A., 1995. Characteritzation of a recombinant human dopamine transporter in multiple cell lines. J. Pharmacol. Exp. Therapeut. 274, 276–283.

Evans, G.J.O., 2018. Subcellular fractionation of the brain: preparation of synaptosomes and synaptic vesicles. CSH Protoc 6.

Ferris, M.J., España, R.A., Locke, J.L., Konstantopoulos, J.K., Rose, J.H., Chen, R., Jones, S.R., 2014. Dopamine transporters govern diurnal variation in extracellular dopamine tone. Proc. Natl. Acad. Sci. U.S.A. 111, E2751–E2759.

Forrest, L.R., Rudnick, G., 2010. The rocking bundle: a mechanism for ion-coupled solute flux by symmetrical transporters. Physiology 377–386.

Foster, J.D., Adkins, S., Lever, J., Vaughan, R., 2008. Phorbol ester induced trafficking-independent regulation and enhanced phosphorylation of the dopamine transporter associated with membrane rafts and cholesterol. J. Neurochem. 105, 1683–1699.

Foster, J.D., Pananusorn, B., Cervinski, M.A., Holden, H.E., Vaughan, R.A., 2003. Dopamine transporters are dephosphorylated in striatal homogenates and in vitro by protein phosphatase 1. Mol. Brain Res. 110, 100–108.

Foster, J.D., Vaughan, R.A., 2017. Phosphorylation mechanisms in dopamine transporter regulation. J. Chem. Neuroanat. 83–84, 10–18.

Foster, J.D., Vaughan, R.A., 2011. Palmitoylation controls dopamine transporter kinetics, degradation, and protein kinase C-dependent regulation. J. Biol. Chem. 286, 5175–5186.

Foster, J.D., Yang, J.W., Moritz, A.E., ChallaSivaKanaka, S., Smith, M.A., Holy, M., Wilebski, K., Sitte, H.H., Vaughan, R.A., 2012. Dopamine transporter phosphorylation site threonine 53 regulates substrate reuptake and amphetamine-stimulated efflux. J. Biol. Chem. 287, 29702–29712.

Gainetdinov, R.R., Fumagalli, F., Jones, S.R., Caron, M.G., 1997. Dopamine transporter is required for in vivo MPTP neurotoxicity: evidence from mice lacking the transporter. J. Neurochem. 69, 1322–1325.

Gao, L., Zhou, W., Symmes, B., Freed, C.R., 2016. Re-cloning the N27 dopamine cell line to improve a cell culture model of Parkinson's disease. PLoS One 1–18.

Garcia-Olivares, J., Torres-Salazar, D., Owens, W.A., Baust, T., Siderovski, D.P., Amara, S.G., Zhu, J., Daws, L.C., Torres, G.E., 2013. Inhibition of dopamine transporter activity by G protein βγ subunits. PLoS One 8, 1–9.

German, C.L., Hanson, G.R., Fleckenstein, A.E., 2012. Amphetamine and methamphetamine reduce striatal dopamine transporter function without concurrent dopamine transporter relocalization. J. Neurochem. 123, 288–297.

Giros, B., Jarber, M., Jones, S.R., Wightman, M., Caron, M.G., 1996. Hyperlocomotion and indifference to cocaine and amphetamine in mice lacking the dopamine transporter. Nature 379, 606–612.

Gluzman, Y., 1981. SV-40 transformed simian cells support the replication of SV40 mutants. Cell 23, 175–182.

Grammatopoulos, T.N., Jones, S.M., Yoshimura, M., Hoover, B.R., Das, M., Snyder, E.Y., Larson, G. a, Zahniser, N.R., Tabakoff, B., Zawada, W.M., 2010. Neurotransplantation of stem cells genetically modified to express human dopamine transporter reduces alcohol consumption. Stem Cell Res. Ther. 1, 36.

Greene, J.G., 2006. Gene expression profiles of brain dopamine neurons and relevance to neuropsychiatric disease. J. Physiol. (London) 575, 411–416.

Greene, L.A., Rein, G., 1977. Release, storage and uptake of catecholamines by a clonal cell line of nerve growth factor (NGF) responsive pheo-chromocytoma cells. Brain Res. 129, 247–263.

Greene, L.A., Tischler, A.S., 1976. Establishment of a noradrenergic clonal line of rat adrenal pheochromocytoma cells which respond to nerve growth factor. Proc. Natl. Acad. Sci. U.S.A. 73, 2424–2428.

Gu, H., Wall, S.C., Rudnick, G., 1994. Stable expression of biogenic amine transporters reveals differences in inhibitor sensitivity, kinetics, and ion dependence. J. Biol. Chem. 269, 7124–7130.

Guptaroy, B., Fraser, R., Desai, A., Zhang, M., Gnegy, M.E., 2011. Site-directed mutations near transmembrane domain 1 alter conformation and function of norepinephrine and dopamine transporters. Mol. Pharmacol. 79, 520–532.

Hahn, M.K., Blakely, R.D., 2002. Monoamine transporter gene structure and polymorphisms in relation to psychiatric and other complex disorders. Pharmacogenomics J. 2, 217–235.

Hamilton, P.J., Belovich, A.N., Khelashvili, G., Saunders, C., Erreger, K., Javitch, J.A., Sitte, H.H., Weinstein, H., Matthies, H.J.G., Galli, A., 2015. PIP2 regulates psychostimulant behaviors through its interaction with a membrane protein. Nat. Chem. Biol. 10, 582–589.

Hanahan, D., Weinberg, R.A., 2011. Hallmarks of Cancer : the next generation. Cell 144, 646–647.

Hara, S., Arawaka, S., Sato, H., Machiya, Y., Cui, C., Sasaki, A., Koyama, S., Kato, T., 2013. Serine 129 phosphorylation of membrane-associated -synuclein modulates dopamine transporter function in a G protein-coupled receptor kinase-dependent

manner. Mol. Biol. Cell 24, 1649–1660.
Hegarty, S.V., Sullivan, A.M., O'Keeffe, G.W., Keeffe, G.W.O., 2013. Midbrain dopaminergic neurons: a review of the molecular circuitry that regulates their development. Dev. Biol. 379, 123–138.
Hong, W.C., Amara, S.G., 2010. Membrane cholesterol modulates the outward facing conformation of the dopamine transporter and alters cocaine binding. J. Biol. Chem. 285, 32616–32626.
Howell, L.L., Wilcox, K.M., 2002. Functional imaging and neurochemical correlates of stimulant self-administration in primates. Psychopharmacology (Berlin) 163, 352–361.
Huang, C.L., Chen, H.C., Huang, N.K., Yang, D.M., Kao, L.S., Chen, J.C., Lai, H.L., Chern, Y., 1999. Modulation of dopamine transporter activity by nicotinic acetylcholine receptors and membrane depolarization in rat pheochromocytoma PC12 cells. J. Neurochem. 72, 2437–2444.
Hull, R.N., Cherry, W.R., Weaver, G.W., 1976. The origin and characteristics of a pig kidney cell strain. LLC-PK. In Vitro 12, 670–677.
Inyushin, M.U., Arencibia-Albite, F., Cruz, A. de la, Vazquez-Torres, R., Colon, K., Sanabria, P., Jimenez-Rivera, C.A., 2013. New method to visualize neurons with DAT in slcies of rat VTA using fluorescent substrate for DAT, ASP+. J Neurosci Neuroeng 6, 98–103.
Iversen, S.D., Iversen, L.L., 2007. Dopamine: 50 years in perspective. Trends Neurosci. 30, 188–193.
Javitch, J.A., Snyder, S.H., 1984. Uptake of MPP(+) by dopamine neurons explains selectivity of parkinsonism-inducing neurotoxin, MPTP. Eur. J. Pharmacol. 106, 455–456.
Jiang, H., Jiang, Q., Feng, J., 2004. Parkin increases dopamine uptake by enhancing the cell surface expression of dopamine transporter. J. Biol. Chem. 279, 54380–54386.
Jones, K.T., Woods, C., Zhen, J., Antonio, T., Carr, K.D., Reith, M.E.A., 2017. Effects of diet and insulin on dopamine transporter activity and expression in rat caudate-putamen, nucleus accumbens, and midbrain. J. Neurochem. 140, 728–740.
Jones, K.T., Zhen, J., Reith, M.E.A., 2012. Importance of cholesterol in dopamine transporter function. J. Neurochem. 123, 700–715.
Kaufman, M.C., Madras, B.K., 1993. [3H]CFT ([3H]win 35,428) accumulation in dopamine regions of monkey brain: comparison of a mature and an aged monkey. Brain Res. 611, 322–325.
Kearns, S.M., Scheffler, B., Goetz, A.K., Lin, D.D., Baker, H.D., Roper, S.N., Mandel, R.J., Steindler, D.A., 2006. A method for a more complete in vitro Parkinson's model: slice culture bioassay for modeling maintenance and repair of the nigrostriatal circuit. J. Neurosci. Meth. 157, 1–9.
Kimmel, H.L., Carroll, F.I., Kuhar, M.J., 2000. Dopamine transporter synthesis and degradation rate in rat striatum and nucleus accumbens using RTI-76. Neuropharmacology 39, 578–585.
Kitayama, S., Shimada, S., Xu, H., Markham, L., Donovan, D.M., Uhl, G.R., 1992. Dopamine transporter site-directed mutations differentially alter substrate transport and cocaine binding. Proc. Natl. Acad. Sci. U.S.A. 89, 7782–7785.
Kivell, B., Uzelac, Z., Sundaramurthy, S., Rajamanickam, J., Ewald, A., Chefer, V., Jaligam, V., Bolan, E., Simonson, B., Annamalai, B., Mannangatti, P., Prisinzano, T.E., Gomes, I., Devi, L.A., Jayanthi, L.D., Sitte, H.H., Ramamoorthy, S., Shippenberg, T.S., 2014. Salvinorin A regulates dopamine transporter function via a kappa opioid receptor and ERK1/2-dependent mechanism. Neuropharmacology 86, 228–240.
Kovalevich, J., Langford, D., 2013. Considerations for the use of SH-SY5Y neuroblastoma cells in neurobiology. Meth. Mol. Biol. 1078, 9–21.
Krishnamurthy, H., Piscitelli, C.L., Gouaux, E., 2009. Unlocking the molecular secrets of sodium-coupled transporters. Nature 459, 347–355.
Kristensen, A.S., Andersen, J., Jørgensen, T.N., Sørensen, L., Eriksen, J., Loland, C.J., Strømgaard, K., 2011. SLC6 neurotransmitter transporters: structure, function, and regulation. Pharmacol. Rev. 63, 585–640.
Krout, D., Rodriquez, M., Brose, S.A., Golovko, M.Y., Henry, L.K., Thompson, B.J., 2017. Inhibition of the serotonin transporter is altered by metabolites of selective serotonin and norepinephrine reuptake inhibitors and represents a caution to acute or chronic treatment paradigms. ACS Chem. Neurosci. 8, 1011–1018.
Lai, T., Yang, Y., Ng, S.K., 2013. Advances in Mammalian cell line development technologies for recombinant protein production. Pharm. Times 6, 579–603.
Lee, F.J.S., Pristupa, Z.B., Ciliax, B.J., Levey, A.I., Niznik, H.B., 1996. The Dopamine Transporter Carboxyl-terminal Tail Truncation/substitution Mutants Selectively Confer High Affinity Dopamine Uptake while Attenuating Recognition of the Ligand Binding Domain. J. Biol. Chem. 20885–20894.
Leighton, J., Estes, L.W., Mansukhani, S., Brada, Z., 1970. A cell line derived from normal dog kidney (MDCK) exhibiting qualities of papillary adenocarcinoma and of renal tubular epithelium. Cancer 26, 1022–1028.
Letchworth, S.R., Nader, M.A., Smith, H.R., Friedman, D.P., Porrino, L., 2001. Progression of changes in dopamine transporter binding site density as a result of cocaine self-administration in rhesus monkeys. J. Neurosci. 21, 2799–2807.
Lew, R., Patel, A., Vaughan, R.A., Wilson, A., Kuhar, M.J., 1992. Microheterogeneity of dopamine transporters in rat striatum and nucleus accumbens. Brain Res. 584, 266–271.
Li, Y., Mayer, F.P., Hasenhuetl, P.S., Burtscher, V., Schicker, K., Sitte, H.H., Freissmuth, M., Sandtner, W., 2017. Occupancy of the zinc-binding site by transition metals decreases the substrate affinity of the human dopamine transporter by an allosteric mechanism. J. Biol. Chem. 292, 4235–4243.
Lin, Z., Itokawa, M., Uhl, G.R., 2000. Dopamine transporter proline mutations influence dopamine uptake, cocaine analog recognition, and expression. Faseb. J. 14, 715–728.
Little, K.Y., Elmer, L.W., Zhong, H., Scheys, J.O., Zhang, L., 2002. Cocaine induction of dopamine transporter trafficking to the plasma membrane. Mol. Pharmacol. 61, 436–445.
Little, K.Y., Kirkman, J.A., Carroll, F.I., Clark, B., Duncan, G.E., 1993. Cocaine use increases [3H]WIN 35428 binding sites in human striatum. Brain Res. 628, 17–25.
Loland, C.J., Desai, R.I., Zou, M., Cao, J., Grundt, P., Gerstbrein, K., Sitte, H.H., Newman, A.H., Katz, J.L., Gether, U., 2008. Relationship between conformational changes in the dopamine transporter and cocaine-like subjective effects of uptake inhibitors. Mol. Pharmacol. 73, 813–823.
Louis, N., Evelegh, C., Graham, F.L., 1997. Cloning and sequencing of the cellular-viral junctions from the human adenovirus type 5 transformed 293 cell line. Virology 233, 423–429.
Lu, Y., Driscoll, N., Ozden, I., Yu, Z., Nurmikko, A.V., 2015. Modulating dopamine release by optogenetics in transgenic mice reveals terminal dopaminergic dynamics. Neurophotonics 2, 031207.
Madras, B.K., Spealman, D., Fahey, M.A., Neumeyer, J.L., Saha, J.K., Milius, R.A., 1989. Cocaine receptors labeled by [3H]2B-carbomethoxy-3B-(1-fluorophenyl)tropane. Mol. Pharmacol. 518–524.
Mash, D.C., Pablo, J., Ouyang, Q., Hearn, W.L., Izenwasse, S., 2002. Dopamine transport function is elevated in cocaine users. J. Neurochem. 81, 292–300.
Mayfield, R.D., Maiya, R., Keller, D., Zahniser, N.R., 2001. Ethanol potentiates the function of the human dopamine transporter expressed in Xenopus oocytes. J. Neurochem. 79, 1070–1079.
Mazei-Robison, M.S., Blakely, R.D., 2005. Expression studies of naturally occurring human dopamine transporter variants identifies a novel state of transporter inactivation associated with Val382Ala. Neuropharmacology 49, 737–749.
Mebel, D.M., Wong, J.C.Y., Dong, Y.J., Borgland, S.L., 2012. Insulin in the ventral tegmental area reduces hedonic feeding and suppresses dopamine concentration via increased reuptake. Eur. J. Neurosci. 36, 2336–2346.
Melikian, H.E., Buckley, K.M., 1999. Membrane trafficking regulates the activity of the human dopamine transporter. J. Neurosci. 19, 7699–7710.
Midde, N.M., Yuan, Y., Quizon, P.M., Sun, W.L., Huang, X., Zhan, C.G., Zhu, J., 2015. Mutations at tyrosine 88, lysine 92 and tyrosine 470 of human dopamine transporter result in an attenuation of HIV-1 tat-induced inhibition of dopamine transport. J. Neuroimmune Pharmacol. 10, 122–135.
Mikelman, S.R., Guptaroy, B., Gnegy, M.E., 2017. Tamoxifen and its active metabolites inhibit dopamine transporter function independently of the estrogen receptors. J. Neurochem. 141, 31–36.
Miller, G.W., Gainetdinov, R.R., Levey, A.I., Caron, M.G., 1999. Dopamine transporters and neuronal injury. Trends Pharmacol. Sci. 20, 424–429.
Moritz, A.E., Foster, J.D., Gorentla, B.K., Mazei-Robison, M.S., Yang, J.W., Sitte, H.H., Blakely, R.D., Vaughan, R.A., 2013. Phosphorylation of dopamine transporter serine 7 modulates cocaine analog binding. J. Biol. Chem. 288, 20–32.
Moritz, A.E., Rastedt, D.E., Stanislowski, D.J., Shetty, M., Smith, M.A., Vaughan, R.A., Foster, J.D., 2015. Reciprocal phosphorylation and palmitoylation control dopamine transporter kinetics. J. Biol. Chem. 290, 29095–29105.
Morón, J. a, Zakharova, I., Ferrer, J.V., Merrill, G. a, Hope, B., Lafer, E.M., Lin, Z.C., Wang, J.B., Javitch, J.a, Galli, A., Shippenberg, T.S., 2003. Mitogen-activated protein kinase regulates dopamine transporter surface expression and dopamine transport capacity. J. Neurosci. 23, 8480–8488.
Nass, R., Hall, D.H., Miller 3rd, D.M., Blakely, R.D., 2002. Neurotoxin-induced degeneration of dopamine neurons in Caenorhabditis elegans. Proc. Natl. Acad. Sci. U.S.A. 99, 3264–3269.
Nirenberg, M.J., Vaughan, R.A., Uhl, G.R., Kuhar, M.J., Pickeli, V.M., 1996. The dopamine transporter is localized to dendritic and axonal plasma membranes of nigrostriatal dopaminergic neurons. J. Neurosci. 76, 436–447.
Patel, A.P., Cerruti, C., Vaughan, R.A., Kuhar, M.J., 1994. Developmentally regulated glycosylation of dopamine transporter. Brain Res Dev 83, 53–58.
Penmatsa, A., Wang, K.H., Gouaux, E., 2015. X-ray structures of Drosophila dopamine transporter in complex with nisoxetine and reboxetine. Nat. Struct. Mol. Biol. 22, 506–508.
Pifl, C., Giros, B., Caron, M.G., 1993. Dopamine transporter expression confers cytotoxicity to low doses of the parkinsonism-inducing neurotoxin 1-methyl-4-phenylpyridinium. J. Neurosci. 13, 4246–4253.
Pifl, C., Hornykiewicz, O., Giros, B., Caron, M.G., 1996. Catecholamine transporters and 1-methyl-4-phenyl-1,2,3,6- tetrahydropyridine neurotoxicity: studies comparing the cloned human noradrenaline and human dopamine transporter. J. Pharmacol. Exp. Therapeut. 277.
Pramod, A.B., Foster, J., Carvelli, L., Henry, L.K., 2013. SLC6 transporters: structure, function, regulation, disease association and therapeutics. Mol. Aspect. Med. 34, 197–219.
Prasad, K.N., Carvalho, E., Kentroti, S., Edwards-Prasad, J., Freed, C., Vernadakis, A., 1994. Establishment and characterization of immortalized clonal cell lines from fetal rat mesencephalic tissue. In Vitro Cell. Dev. Biol. Anim. 30A, 596–603.
Ramamoorthy, S., Shippenberg, T.S., Jayanthi, L.D., 2011. Regulation of monoamine transporters: role of transporter phosphorylation. Pharmacol. Ther. 129, 220–238.
Rao, A., Sorkin, A., Zahniser, N.R., 2013. Mice expressing markedly reduced striatal dopamine transporters exhibit increased locomotor activity, dopamine uptake turnover rate and cocaine responsiveness. Synapse 67, 668–677.
Rastedt, D.E., Vaughan, R.A., Foster, J.D., 2017. Palmitoylation mechanisms in dopamine transporter regulation. J. Chem. Neuroanat. 83–84, 3–9.
Reith, M.E.A., Ali, S., Hashim, A., Sheikh, I.S., Theddu, N., Gaddiraju, N.V., Mehrotra, S., Schmitt, K.C., Murray, T.F., Sershen, H., Unterwald, E.M., Davis, F.A., 2012. Novel C-1 substituted cocaine analogs unlike cocaine or benztropine. J. Pharmacol. Exp. Therapeut. 343, 413–425.
Richards, T.L., Zahniser, N.R., 2009. Rapid substrate-induced down-regulation in function and surface localization of dopamine transporters: rat dorsal striatum versus nucleus accumbens. J. Neurochem. 1575–1584.
Robbins, A., Horlick, R., 1998. Macrophage scavenger receptor confers an adherent phenotype to cells in culture. Biotechniques 2, 240–244.

Sabeti, J., Adams, C.E., Burmeister, J., Gerhardt, G.A., Zahniser, N.R., 2002. Kinetic analysis of striatal clearance of exogenous dopamine recorded by chronoamperometry in freely-moving rats. J. Neurosci. Meth. 121, 41–52.
Safratowich, B.D., Hossain, M., Bianchi, L., Carvelli, L., 2014. Amphetamine potentiates the effects of B-phenylethylamine through activation of an amine-gated chloride channel. J. Neurosci. 34, 4686–4691.
Salto, R., Vilchez, J.D., Giron, M.D., Cabrera, E., Campos, N., Manzano, M., Rueda, R., Lopez-Pedrosa, J.M., 2015. Beta-hydroxy-beta-methylbutyrate (HMB) promotes neurite outgrowth in Neuro2a cells. PLoS One 10.
Schmitt, K.C., Reith, M.E.A., 2011. The atypical stimulant and nootropic modafinil interacts with the dopamine transporter in a different manner than classical cocaine-like inhibitors. PLoS One 6.
Shaw, G., Morse, S., Ararat, M., Graham, F.L., 2002. Preferential transformation of human neuronal cells by human adenoviruses and the origin of HEK 293 cells. FASEB J. 16, 869–871.
Shimamura, T., Weyand, S., Beckstein, O., Rutherford, N.G., Hadden, J.M., Sharples, D., Sansom, M.S.P., Iwata, S., Henderson, P.J.F., Cameron, A.D., 2010. Molecular basis of alternating access membrane transport by the sodium-hydantoin transporter Mhp1. Science (Wash. D C) 328, 470–473.
Sidhu, A., 1997. Regulation and expression of D-1 but not D-5, dopamine receptors in human SK-N-MC neuroblastoma cells. J. Recept. Signal Transduct. Res. 5, 777–784.
Slusher, B.S., Tiffany, C.W., Olkowski, J.L., Jackson, P.F., 1997. Use of identical assay conditions for cocaine analog binding and dopamine uptake to identify potential cocaine antagonists. Drug Alcohol Depend. 48, 43–50.
Speed, N., Saunders, C., Davis, A.R., Owens, W.A., Matthies, H.J.G., Saadat, S., Kennedy, J.P., Vaughan, R.A., Neve, R.L., Lindsley, C.W., Russo, S.J., Daws, L.C., Niswender, K.D., Galli, A., 2011. Impaired striatal akt signaling disrupts dopamine homeostasis and increases feeding. PLoS One 6, 1–10.
Staley, J.K., Hearn, W.L., Ruttenber, A.J., Wetli, C.V., Mash, D.C., 1994. High affinity cocaine recognition sites on the dopamine transporter are elevated in fatal cocaine overdose victims. J. Pharmacol. Exp. Therapeut. 271, 1678–1685.
Sulzer, D., Sonders, M.S., Poulsen, N.W., Galli, A., 2005. Mechanisms of neurotransmitter release by amphetamines: a review. Prog. Neurobiol. 75, 406–433.
Sweeney, C.G., Tremblay, B.P., Stockner, T., Sitte, H.H., Melikian, H.E., 2017. Dopamine transporter amino and carboxyl termini synergistically contribute to substrate and inhibitor affinities. J. Biol. Chem. 292, 1302–1309.
Tang, Q.Y., Kolanos, R., De Felice, L.J., Glennon, R.A., 2015. Structural analysis of dopamine- and amphetamine-induced depolarization currents in the human dopamine transporter. ACS Chem. Neurosci. 6, 551–558.
Tremblay, R.G., Sikorska, M., Sandhu, J.K., Lanthier, P., Ribecco-Lutkiewicz, M., Bani-Yaghoub, M., 2010. Differentiation of mouse Neuro 2A cells into dopamine neurons. J. Neurosci. Meth. 186, 60–67.
Vaughan, R.A., Foster, J.D., 2013. Mechanisms of dopamine transporter regulation in normal and disease states. Trends Pharmacol. Sci. 34, 489–496.
Vaughan, R.A., Huff, R.A., Uhl, G.R., Kuhar, M.J., 1997. Protein kinase C-mediated phosphorylation and functional regulation of dopamine transporters in striatal synaptosomes. J. Biol. Chem. 272, 15541–15546.
Vickrey, T.L., Xiao, N., Venton, B.J., 2013. Kinetics of the dopamine transporter in Drosophila larva. ACS Chem. Neurosci. 4, 832–837.
Volz, T.J., Farnsworth, S.J., Hanson, G.R., Fleckenstein, A.E., 2009. Measurement of plasmalemmal dopamine transport, vesicular dopamine transport, and K+-stimulated dopamine release in frozen rat brain tissue. J. Neurosci. Meth. 180, 317–320.
Wang, L.C., Cui, X.N., Chen, N., Reith, M.E.A., 2003. Binding of cocaine-like radioligands to the dopamine transporter at 37°C: effect of Na+ and substrates. J. Neurosci. Meth. 131, 27–33.
Wang, W., Runkle, K.B., Terkowski, S.M., Ekaireb, R.I., Witze, E.S., 2015. Protein depalmitoylation is induced by Wnt5a and promotes polarized cell behavior. J. Biol. Chem. 290, 15707–15716.
Wheeler, D.S., Ebben, A.L., Kurtoglu, B., Lovell, M.E., Bohn, A.T., Jasek, I.A., Baker, D.A., Mantsch, J.R., Gasser, P.J., Wheeler, R.A., 2017. Corticosterone regulates both naturally occurring and cocaine-induced dopamine signaling by selectively decreasing dopamine uptake. Eur. J. Neurosci. 46, 2638–2646.
Wheeler, D.S., Underhill, S.M., Stolz, D.B., Murdoch, G.H., Thiels, E., Romero, G., Amara, S.G., 2015. Amphetamine activates Rho GTPase signaling to mediate dopamine transporter internalization and acute behavioral effects of amphetamine. Proc. Natl. Acad. Sci. U.S.A. 112, E7138–E7147.
Whittaker, V., Michaelson, I., Kirkland, R., 1964. The separation of synaptic vesicles from nerve-ending particles ('synaptosomes'). Biochem. J. 90, 293–303.
Woolverton, W.L., Rowlett, J.K., Wilcox, K.M., Paul, I.A., Kline, R.H., Newman, A.H., Katz, J.L., 2000. 3'- and 4'-chloro-substituted analogs of benztropine: intravenous self-administration and in vitro radioligand binding studies in rhesus monkeys. Psychopharmacology (Berlin) 147, 426–435.
Wu, S., Fagan, R.R., Uttamapinant, C., Lifshitz, L.M., Fogarty, K.E., Ting, A.Y., Melikian, H.E., 2017. The dopamine transporter recycles via a retromer-dependent post-endocytic mechanism: tracking studies using a novel fluorophore-coupling approach. J. Neurosci. 37 3885–16.
Wu, X., Gu, H.H., 1999. Molecular cloning of the mouse dopamine transporter and pharmacological comparison with the human homologue. Gene 233, 163–170.
Wurm, F.M., 2004. Production of recombinant protein therapeutics in cultivated mammalian cells. Nat. Biotechnol. 22, 1393–1398.
Xicoy, H., Wieringa, B., Martens, G.J., 2017. The SH-SY5Y cell line in Parkinson's disease research: a systematic review. Mol. Neurodegener. 12, 10.
Yuan, Y., Quizon, P.M., Sun, W.L., Yao, J., Zhu, J., Zhan, C.G., 2016. Role of histidine 547 of human dopamine transporter in molecular interaction with HIV-1 tat and dopamine uptake. Sci. Rep. 6, 1–10.
Zahniser, N.R., Larson, G.A., Gerhardt, G.A., 1999. In vivo dopamine clearance rate in rat striatum: regulation by extracellular dopamine concentration and dopamine transporter inhibitors. J. Pharmacol. Exp. Therapeut. 289, 266–277.
Zeppelin, T., Ladefoged, L.K., Sinning, S., Periole, X., Schiøtt, B., 2018. A direct interaction of cholesterol with the dopamine transporter prevents its out-to-inward transition. PLoS Comput. Biol. 14, 1–24.
Zhang, L., Elmer, L., Little, K.Y., 1998. Expression and regulation of the human dopamine transporter in a neuronal cell line. Brain Res Mol Brain Res 59, 66–73.
Zhen, J., Antonio, T., Cheng, S.Y., Ali, S., Jones, K.T., Reith, M.E.A., 2015. Dopamine transporter oligomerization: impact of combining protomers with differential cocaine analog binding affinities. J. Neurochem. 133, 167–173.
Zhen, J., Chen, N., Reith, M.E.A., 2005. Differences in interactions with the dopamine transporter as revealed by diminishment of Na+ gradient and membrane potential: dopamine versus other substrates. Neuropharmacology 49, 769–779.
Zhen, J., Reith, M.E.A., 2016. Impact of disruption of secondary binding site S2 on dopamine transporter function. J. Neurochem. 138, 694–699.
Zhu, S.J., Kavanaugh, M.P., Sonders, M.S., Amara, S.G., Zahniser, N.R., 1997. Activation of protein kinase C inhibits uptake, currents and binding associated with the human dopamine transporter expressed in Xenopus oocytes. J. Pharmacol. Exp. Therapeut. 282, 1358–1365.